

Direct observation of fermion spin superposition by neutron interferometry

J. Summhammer, G. Badurek, and H. Rauch

Atominstitut der Österreichischen Universitäten, Schüttelstrasse 115, A-1020 Wien, Austria

U. Kischko

Institut Laue-Langevin, F-38042 Grenoble, France

and Institut für Physik, Universität Dortmund, D-4600 Dortmund, Federal Republic of Germany

A. Zeilinger

Department of Physics, Massachusetts Institute of Technology, Cambridge, Massachusetts 02139

(Received 10 November 1982)

The coherent superposition of oppositely polarized neutron beams of equal amplitude results in a final beam polarization perpendicular to the polarization of both initial beams. This polarization can be rotated by purely scalar interaction applied to the beams before superposition, which is equivalent to an additional Larmor precession applied to the beam after superposition. We have directly observed these effects in an experiment performed using the perfect-crystal neutron interferometer at the high-flux reactor at Grenoble. This paper gives the experimental results and discusses their theoretical foundation.

I. INTRODUCTION

Single-crystal interferometers for use with thermal neutrons have opened many possibilities during the course of their refinement.¹ The relatively large separation of the two coherent partial beams in the order of several centimeters permits the manipulation of one of the beams without much affecting the other. Thus, wherever information can be obtained by the influence of a specimen on the phase of the neutron wave function, the interferometer may be a convenient tool of research. Today the interferometer is routinely used for precision measurements of coherent neutron-nucleus scattering lengths. Measurements on solids, liquids, and gases have been performed.²⁻⁴

Besides these applications another class of experiments has become possible where the quantum-mechanical behavior of the neutron itself is investigated. Collela *et al.*⁵ reported on a measurement showing the influence of the gravitational term in the Hamiltonian; Rauch *et al.*^{6,7} and Werner *et al.*⁸ could independently demonstrate the change of sign of the neutron wave function when subjected to 2π rotations. Combined effects of nuclear and magnetic phase shifts were observed by Badurek *et al.*⁹ These latter experiments exhibit some of the consequences of the fact that the neutron is a fermion of

spin $\frac{1}{2}$, and therefore its wave function is a spinor. These experiments could be performed with an unpolarized incident neutron beam. The experiment presented here belongs to this category, although it requires a polarized incident beam. The purpose of our research was a demonstration of the phenomena encountered when two coherent neutron beams of opposite spin eigenstates (of polarization direction parallel and antiparallel to the magnetic guide field) are superposed. Quantum theory predicts that the resulting beam would not be a mixture as one might intuitively visualize in a classical picture. Instead, one expects the final polarization vector to lie in a plane perpendicular to the initial polarization directions.

The first suggestion for a similar experiment was made, although on the *gedanken* level, by Wigner in an article on the problem of measurement in quantum theory.¹⁰ More recently, Eder and Zeilinger suggested its realization^{11,12} by neutron interferometry and showed that the particular direction of the polarization vector within the plane mentioned above can be modified by introducing a scalar phase shift between the two constituent beams. Some preliminary results of the measurements have already been reported.¹³ Here a detailed description of the experiment, of the theoretical formalism, and of the presentation of the results is given.

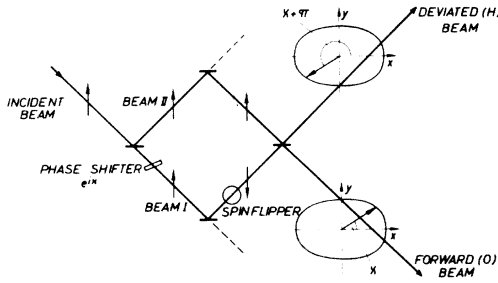


FIG. 1. Experimental test of spin superposition: rotation of the polarization vectors in the beams leaving the interferometer by a nuclear phase shift.

II. THEORETICAL CONSIDERATIONS

In order to obtain two beams of opposite spin states we choose to illuminate the interferometer with polarized neutrons and to invert the spin state of one of the coherent beams with respect to the other. In addition, a scalar phase shift can be introduced. A sketch of the principles of such an experiment is seen in Fig. 1. For our purposes the interaction of the beam with the interferometer can be considered to be equivalent to one consisting of semi-transparent mirrors, where each reflection adds a phase factor of $\exp(i\pi/2)$ to the reflected wave function. The inversion of the spin state in one beam is formally a rotation of π rad, whereas the scalar phase shift gives the phase factor $\exp(i\chi)$. The phase χ is given by the index of refraction n , which for purely nuclear interaction is $n = (1 - \bar{V}/E)^{1/2} \sim 1 - \lambda^2 N b_c / 2\pi$. Thus $\chi = -k(1-n)\Delta D = -N\lambda b_c \Delta D$, where λ is the neutron wavelength, N is the number of nuclei per unit volume, b_c is the coherent neutron-nucleus scattering length, k is the vacuum wave number of the neutrons, and ΔD is the effective thickness of the phase-shifter plate. Assuming incident neutrons of the $|\uparrow_z\rangle$ state and a 180° rotation around the y axis, the result of the superposition in the forward beam after the interferometer can be written (using the notation of Ref. 12) as

$$\begin{aligned} |0\rangle &= \frac{1}{2} |\uparrow_z\rangle + \frac{1}{2} e^{i\chi} e^{-i\sigma_y \pi/2} |\uparrow_z\rangle \\ &= \frac{1}{2} |\uparrow_z\rangle + \frac{1}{2} e^{i\chi} |\downarrow_z\rangle \\ &= \frac{e^{i\chi/2}}{\sqrt{2}} \left[\cos \frac{\chi}{2} |\uparrow_x\rangle - i \sin \frac{\chi}{2} |\downarrow_x\rangle \right], \end{aligned} \quad (1)$$

where σ_y is the y component of the vector of the

Pauli spin matrices, $\vec{\sigma} = (\sigma_x, \sigma_y, \sigma_z)$. One observes from Eq. (1) that the polarization of this beam can be rotated by a purely scalar interaction. Of course, the conservation law of angular momentum is not violated, since the total wave function includes the deviated beam, whose spin is always opposite to that of the forward beam

$$\begin{aligned} |H\rangle &= \frac{1}{2} |\uparrow_z\rangle + \frac{1}{2} e^{i\pi} e^{i\chi} e^{-i\sigma_y \pi/2} |\uparrow_z\rangle \\ &= \frac{1}{2} |\uparrow_z\rangle - \frac{1}{2} e^{i\chi} |\downarrow_z\rangle \\ &= \frac{e^{i\chi/2}}{\sqrt{2}} \left[\cos \frac{\chi}{2} |\downarrow_x\rangle - i \sin \frac{\chi}{2} |\uparrow_x\rangle \right]. \end{aligned} \quad (2)$$

The polarization of the interferometric beams I and II before superposition is antiparallel and parallel to the z direction, respectively,

$$\begin{aligned} \vec{P}_I &= \langle \downarrow_z | \vec{\sigma} | \downarrow_z \rangle = (0, 0, -1), \\ \vec{P}_{II} &= \langle \uparrow_z | \vec{\sigma} | \uparrow_z \rangle = (0, 0, +1). \end{aligned} \quad (3)$$

In contrast, the polarization of the beams in forward and deviated directions is obtained to be

$$\begin{aligned} \vec{P}_0 &= \langle 0 | \vec{\sigma} | 0 \rangle = (\cos \chi, \sin \chi, 0), \\ \vec{P}_H &= \langle H | \vec{\sigma} | H \rangle = (-\cos \chi, -\sin \chi, 0). \end{aligned} \quad (4)$$

There is no z component in the polarization vectors, but they have length 1 and point in directions in the x - y plane which depend on the scalar phase shift. This is opposed to the properties of a statistical mixture, which would render completely unpolarized beams. Thus by means of three-dimensional polarization analysis the two cases can be distinguished.

III. PRINCIPLE OF THE EXPERIMENT

The experimental setup is sketched in Fig. 2. A monochromatic but unpolarized beam propagates in the y direction and passes the air gap of an electromagnet with prism-shaped poles. Owing to their magnetic moment the neutrons of the spin-up state ($|\uparrow_z\rangle$) experience a different deflection than those of the spin-down state ($|\downarrow_z\rangle$). With strong laboratory fields an angular separation in the order of several seconds of arc, which is larger than the intrinsic reflection half-width of the nondispersive monochromator-interferometer arrangement, can be achieved.^{14,15} Thus by appropriate adjustment of the interferometer only one of the polarized subbeams can be made to fulfill the Bragg condition. The other one passes the first and second slab of the interferometer virtually without any reflection and is lost. Thus there are neutrons of only one spin direction for use in the interferometer. The axis of quantization as defined by the direction of the mag-

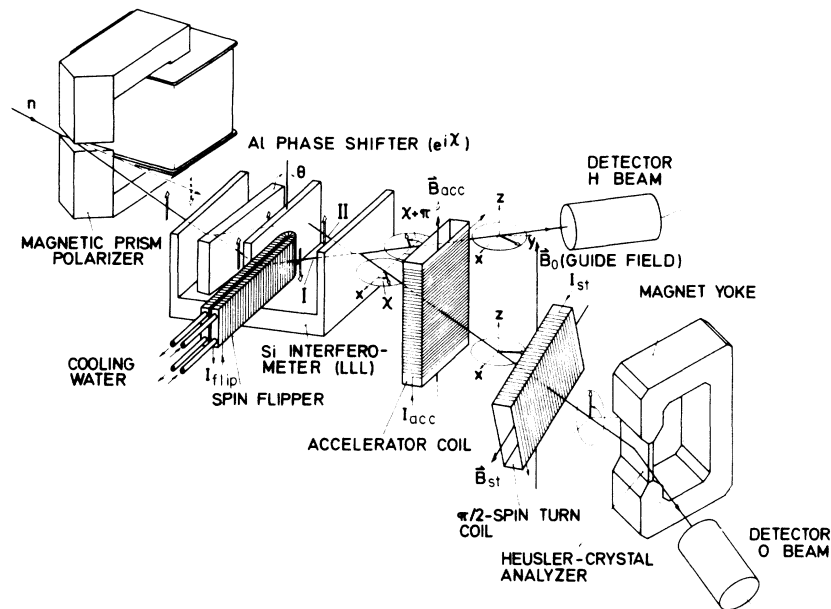


FIG. 2. Schematic of the experiment for spin superposition.

netic field of the prism is kept over the whole experimental arrangement by exposing it to a vertical magnetic guide field ($+z$ direction). In the first spacing of the interferometer a relative scalar phase shift χ is introduced between the two coherent beams I and II by means of a plane slab of Al with parallel faces. In the second spacing the polarization direction of beam I is inverted by a miniaturized dc spin flipper.¹⁶⁻¹⁸

In the ideal case the wave functions corresponding to interferometric beams I and II represent the two different spin eigenstates of the neutrons in the magnetic guide field. Therefore as a result of the superposition in the third slab the wave functions of the forward and deviated beam describe no longer eigenstates in the magnetic field. Consequently, their corresponding polarization vectors precess with the Larmor frequency around the direction of the guide field. In the experiment only the polarization of the O beam was investigated. Following its path the neutrons first pass the accelerator coil which produces a variable magnetic field parallel to the guide field. The Larmor frequency within the coil can be varied by changing the current. Thus the polarization vector can be turned by an additional angle α and can be made to assume any desired direction in the x - y plane. In particular, if the polarization vector points in the y direction at the entrance of the $\pi/2$ -spin turn coil, which turns the vector around the x axis by 90° , the final polarization points in $-z$

direction. Finally, the Heusler single-crystal analyzer reflects only that part of the intensity which corresponds to a polarization parallel to $+z$. So in this case there will be a minimum of the intensity behind the analyzer. On the other hand, if the current of the accelerator coil is adjusted in such a way that the polarization vector behind the $\pi/2$ coil points in the $+z$ direction, a maximum of the intensity occurs. Therefore one will find a sinusoidal dependence of the intensity on the current of the accelerator coil. As can be seen from Eq. (4), the polarization vector can also be turned by a scalar phase shift introduced between beams I and II. This equivalence of scalar phase shift within and magnetic spin-dependent phase shift (Larmor precession) behind the interferometer can only be attributed to coherent spin superposition. A formal description of the experimental scheme is given in the Appendix.

IV. EXPERIMENTAL SETUP

The experiment was performed at the neutron interferometer setup at the high-flux reactor in Grenoble. Its layout is shown in Fig. 2. Differing from this figure two magnetic prisms were used in series, each having an air gap of 4.5 mm in height and a refractive angle of 120° . At saturation magnetization fields of ≤ 0.8 T were measured in the air gaps which resulted in a total beam separation of 3.9 sec

of arc. The mean wavelength of the incident beam was determined as $\lambda = 1.835(2) \text{ \AA}$. The guide field was produced by a Helmholtz configuration of 620 mm in diameter whose center of symmetry coincided with that of the beams inside the interferometer. The distance of the second magnetic prism was about 350 mm from the interferometer. The total magnetic field at the site of the crystal was 4 mT.

The accelerator coil and the $\pi/2$ coil were solenoids of 220-mm length, 60-mm width, and 11-mm effective thickness along the beam trajectory. The $\pi/2$ coil was tilted by an angle of 27° from the vertical, and the current was tuned so that its field together with that of the Helmholtz coils gave a resulting field direction within the x - y plane. The stray field of the coils was not larger than 0.09 mT anywhere on the neutron beam paths. The important spin flipper within the interferometer was of the dc type. It was a solenoid bent to form a "U," ensuring the desired field at the site of beam I and negligible stray field along the path of beam II, although the maximum separation of the beams was only 20 mm.¹⁸ Since a homogeneous field over the cross section required beam I to pass through wires, and since the coherence properties, i.e., equal nuclear phase shift over the cross section had to be maintained, the material of the wire had to have an index of refraction $n = 1$. This condition was met by a homogeneous alloy of $\text{Nb}_{5.4}\text{V}_{94.6}$. Cooling with temperature-controlled water was necessary to dissipate the 35 W of heat produced thus directly inside the interferometer. As the wire was 1 mm in diameter and the thickness of each field region was only 5 mm, the condition of equal angle of rotation over the cross section of the beam could not be fulfilled completely. We estimate, that this, and deviations of the alloy from the ideal composition, were the main reasons for the reduction of the contrast of the intensity oscillations in the 0 beam. Furthermore, different effective lengths of the two parts of the spin flipper along the neutron path and different effective fields in them gave rise to the incomplete spin turn (see the Appendix). The entrance slit placed in front of the interferometer defined a cross section of the incident beam of $2 \times 4 \text{ mm}^2$. Owing to the Borrmann fan the beams are widened noticeably after the first slab (thickness 4.5 mm), so that for reasons of space a spin flip of a wider beam could not have been accomplished.

V. RESULTS

A. Polarization of beams I and II

For measurements of the polarizations of the individual beams phase shifter, accelerator coil, and $\pi/2$

coil were not present. A Cd beamstop was placed either in the path of beam I or that of beam II right before the second slab. By turning the interferometer around θ first the subbeam with negative, then the one with positive polarization fulfills the Bragg condition. Thus the rocking curve gives two peaks in the H detector (see Fig. 3). In the 0 detector a different result is obtained because of the Heusler analyzer present. If the neutrons have followed the path of beam I, either the first or the second peak appears depending on whether the spin flipper is on or off. For a nonideal spin flip a small peak at the position of the supposedly suppressed one is found. If the neutrons have passed via beam II, the rocking curves should be the same independent of whether the spin flipper is on or off. The results in Fig. 3 show that its stray fields do only have a small influence on beam II. With the interferometer positioned on the subbeam with positive polarization for the case of "flipper on" a polarization of $P_1^z = P_i D_p F D_H \leq -0.87$ for beam I and $P_{II}^z = P_i D_p D_F D_H \geq 0.81$ for beam II was found. Here $P_i = 0.95$ is the theoretical maximum polarization; its value is due to an overlap of the individual rocking curves of the incident subbeams. D_p is a possible depolarization along the flight path, which is small and thus we set $D_p = 1$. The factor D_H accounts for a quasidepolarization by the Heusler analyzer as its reflectivity for the $|\downarrow_z\rangle$ state was $\leq 3\%$ of that of the $|\uparrow_z\rangle$ state and hence $D_H \geq 0.94$. Finally, the value for beam I contains the efficiency of the spin flipper $F = 2\delta^2 - 1$ which was measured as $F \leq -0.98$. From this a value of $\delta \sim 0.1$ can be extracted [see Eq. (A9)]. For beam II a factor $D_F \geq 0.91$ describing a small depolarizing effect of the stray field of the spin flipper has to be included. Considering all disturbing influences it could therefore be assumed that there are mainly neutrons of the $|\downarrow_z\rangle$ state in beam I and of the $|\uparrow_z\rangle$ state in beam II.

B. Spin superposition

Since the objective was to measure the intensity as a function of the scalar phase shift χ and the additional Larmor angle α , the angular position of the phase plate was incremented in steps, at each step determining the count rates in the detectors for a series of currents in the accelerator coil. These scans were performed for both positive and negative incident polarization. Typical results can be seen in Fig. 4. The sinusoidal curves were obtained applying a least-squares fit to a set of data points belonging to a fixed current in the accelerator coil (fixed α). The formula

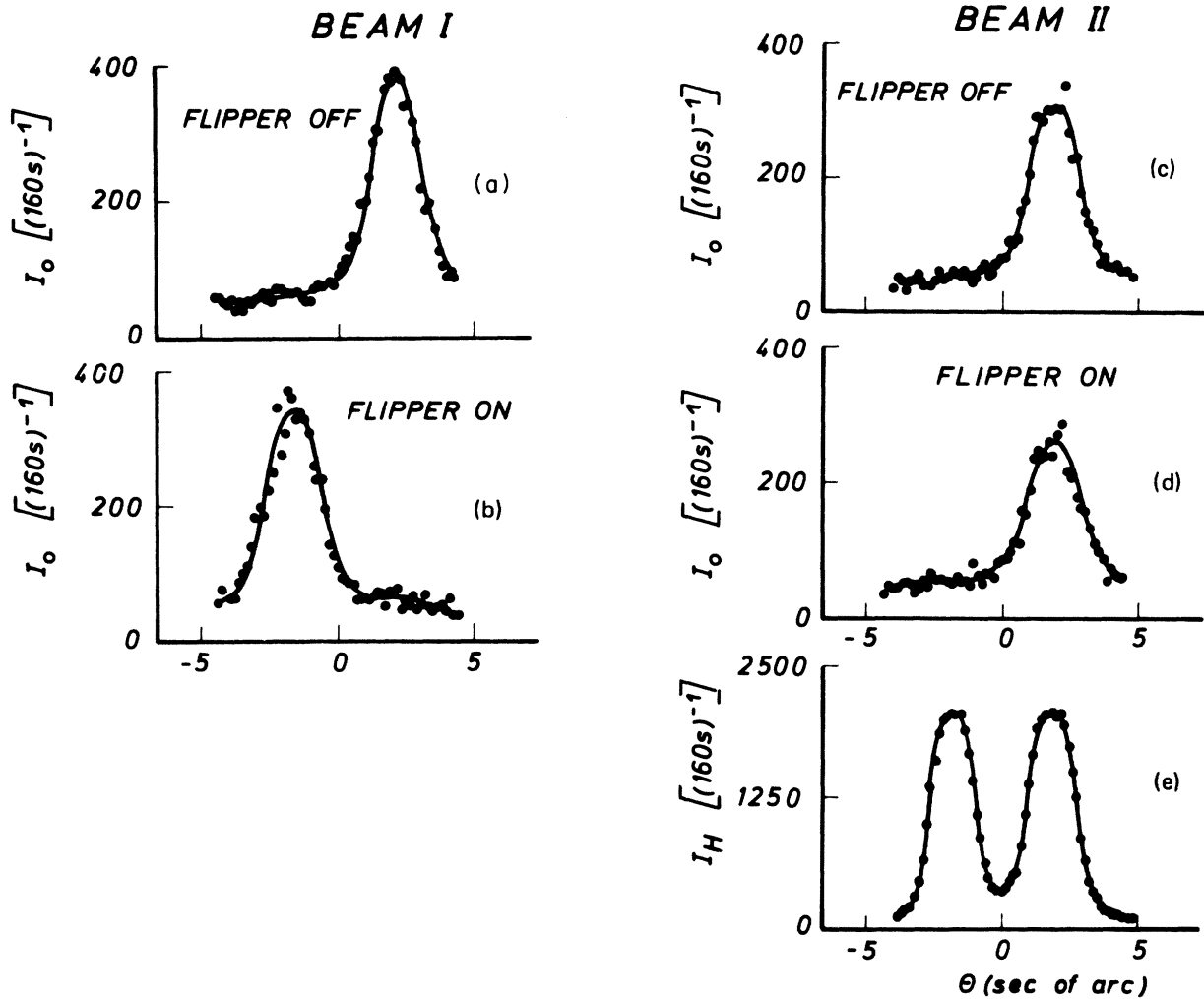


FIG. 3. Rocking curves of the interferometer crystal to determine the polarization of beams I and II in the interferometer. Deviated (H) beam: without polarization analysis two peaks occur, corresponding to the two incident subbeams (e). Principal shape of the curve is independent of whether beam I or beam II is blocked off, or whether the flipper is on or off. Forward (0) beam: only that peak is present which is caused by neutrons of the $|\uparrow_z\rangle$ state. Beam I [beam II in the interferometer blocked off, (a) and (b)]: with "flipper off" the incident subbeam with neutrons of the $|\uparrow_z\rangle$ state gives the peak, whereas with "flipper on" it is the incident subbeam with neutrons of the $|\downarrow_z\rangle$ state, because the spin is inverted. Beam II [beam I in the interferometer blocked off (c) and (d)]: only the incident subbeam with neutrons of the $|\uparrow_z\rangle$ state gives a peak. Action of the spin flipper has no influence.

$$I_0(\Delta D) = T_1 + T_2 \cos[2\pi(\Delta D/T_3 + T_4)] \quad (5)$$

was used, optimizing the parameters T_1, \dots, T_4 . Here T_1 is the mean intensity. It includes also an incoherent part due to imperfections and temperature gradients in the interferometer crystal as well as some small-angle scattering in the wire of the spin flipper. T_2 is the amplitude of the intensity oscillations. The quotient T_2/T_1 gives the interferometric contrast, which is 1 for the 0 beam in an idealized

experiment, but in our experiment it was only 0.05–0.1. T_3 denotes the λ thickness of the aluminum plate that causes a relative phase shift of 2π in between beams I and II and which is given as $T_3 = 2\pi/N\lambda b_c$. Its value was known from many previous experiments on scattering lengths as $T_3 = 164.9 \mu\text{m}$, and it could thus serve as a control.² Here typical values of $T_3 = 160 \pm 9 \mu\text{m}$ were obtained. T_4 is the phase which was expected to depend linearly on the Larmor angle α . The dashed

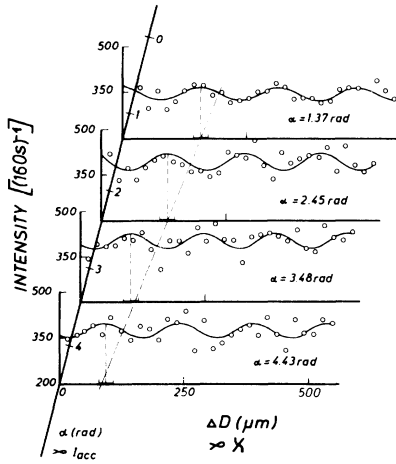


FIG. 4. Results of spin superposition in forward direction. The phase of the intensity oscillations is a function of the path difference ΔD in the Al phase shifter of beams I and II as well as of the current I_{acc} in the accelerator coil.

line in Fig. 4 indicates this relationship as it was found in the experiment. The slope of the line is in good agreement with the theoretical value computed from coil parameters and wavelength λ (see Table I). It could also be observed that the sign of the slope changes if the incident polarization is reversed with the experimental procedure otherwise remaining the same.

From Fig. 4 one notices that the mean intensity T_1 , too, is a periodic function of the additional Larmor angle α . This effect is caused by an incomplete spin flip (see the Appendix). That its amplitude is larger than T_2 is due to the noninterfering part of the intensity.

A further verification, that the observed intensity oscillations in the 0 detector as a function of the phase shift χ were indeed due to a rotation of the polarization vector, was done by switching off the $\pi/2$ coil. Then the intensity should not depend on χ . Results of this experiment are shown in Fig. 5.

VI. DISCUSSION

The results show that the creation and coherent superposition of neutron beams of such different physical property as opposite spin can be achieved by interferometry. Repeated experiments have demonstrated a very good agreement of the observed phenomena with the quantum-theoretical predictions, despite an error of the relevant phases ($2\pi T_4$) of up to $(\pm 0.09) \times 2\pi$ (see error bars in Fig. 4).

TABLE I. Comparison of theoretical and experimental dependence of the absolute phase of the intensity oscillations in Fig. 4 on the Larmor angle α . (Measured values have been corrected to give the theoretical phase at $\alpha = \pi$.)

Theoretical phase (rad)	Measured phase (rad)
1.37	1.80 ± 0.56
2.45	2.53 ± 0.55
3.48	3.53 ± 0.69
4.43	4.06 ± 0.75

With an improvement of accuracy experiments will become feasible that not only demonstrate this special case of the superposition principle, but permit a more quantitative analysis as well. In one experiment, for example, a partial absorber was placed in one beam path inside the interferometer diminishing the amplitude of the corresponding spinor. According to Ref. 12, by changing the effective absorption and by varying the nuclear phase shift with the aluminum slab one should be able to produce any direction in three-dimensional space of the polarization vectors of the outgoing beams, although both controlling interactions are spin independent. Owing to the rather large experimental error these measurements did not render decisive results and will be

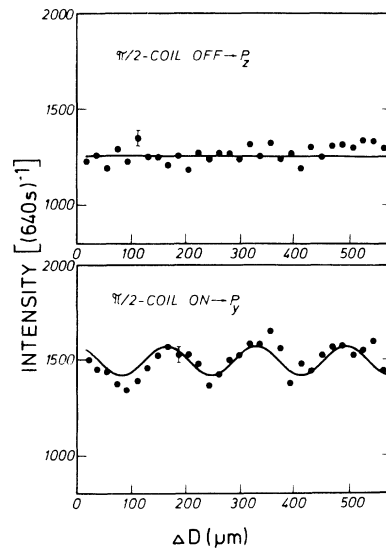


FIG. 5. Spin superposition in forward direction. Intensity oscillations as a function of the path difference ΔD (phase χ) are only present when the polarization of the y direction is turned into the z direction, indicating the influence of the nuclear phase shift on the final polarization.

repeated.

An additional effect inherent in our experiment must be mentioned. As is known from dynamical diffraction theory,¹⁹⁻²¹ the direction of propagation of neutrons inside a single crystal is influenced strongly by changes of wavelength, if the incident beam is near the Bragg condition and if Laue geometry is used, as in the interferometer.²² But neutrons of the same total energy and of opposite spin eigenstates in a constant magnetic field have different momentum and consequently different wavelength. In our experiment this meant that neutrons of beam I, which experienced a spin flip and thus a change of wavelength, had different direction of propagation in the third crystal slab as compared to the first and second slabs, while for neutrons of

beam II no such change occurred. As a consequence, the coherence of beams I and II was reduced, a small effect that could be observed. It could not be completely eliminated, as a guide field was necessary for the definition of the spin states.

A possibility of circumventing wavelength differences is the use of an rf spin flipper instead of the static one. The total energy of the neutrons whose spin is inverted is then given by $E_0 \pm \hbar\omega_{\text{rf}}$, where $\hbar\omega_{\text{rf}}$ is the energy of the photons emitted or absorbed by the rf coil.^{23,24} It corresponds to the energy difference of the Zeeman levels of a neutron in a magnetic field, and thus the kinetic energy remains the same. Using calculations given in Ref. 25 the state of the 0 beam behind the interferometer is obtained to be with incident neutrons of the $|\uparrow_z\rangle$ state,

$$|0\rangle = \frac{1}{2} |\uparrow_z\rangle + e^{i\chi} e^{-i\omega_{\text{rf}}t} |\downarrow_z\rangle = \frac{e^{i(\chi - \omega_{\text{rf}}t)/2}}{\sqrt{2}} \left[\cos \left[\frac{\chi - \omega_{\text{rf}}t}{2} \right] |\uparrow_x\rangle - i \sin \left[\frac{\chi - \omega_{\text{rf}}t}{2} \right] |\downarrow_x\rangle \right]. \quad (6)$$

For a magnetic guide field in the order of 10 mT $\omega_{\text{rf}}/2\pi \sim 10^5$ Hz. Because of the explicit time dependence of the resulting intensity, neutron detection must be synchronized with the phase of the rf field. Such measurements will be performed in the near future. Yet without doubt they will show the same properties of spin superposition as our results for the dc case.

ACKNOWLEDGMENTS

Fruitful discussions with Professor E. Balcar and Professor G. Eder (Atominstut Vienna), Dr. F. Mezei (of the Institute Laue-Langevin at Grenoble), and Professor S. A. Werner (of Columbia University) are gratefully acknowledged. The authors wish also to thank P. Pataki and K. Zeitler (Atominstut Vienna) and notably G. Schmidt (of the Institut Laue-Langevin at Grenoble), for technical assistance. This work has been supported financially by the Austrian Fonds zur Förderung der wissenschaftlichen Forschung (Project No. 4230) and by the Bundesminister für Forschung und Technologie, Bonn (Forschungsbereich No. 03-41E09P).

APPENDIX: FORMAL TREATMENT OF THE EXPERIMENTAL SCHEME

1. Incident beam

For monochromatization the (220) reflection of a perfect silicon crystal in Bragg setting is used.

There are no magnetic fields acting on it. Thus a spin-independent momentum in vacuum $\vec{p} = \hbar\vec{k}$ is defined, the total energy of the neutrons being $E_0 = (\hbar k)^2/2m$ (where m is the mass of neutron). The magnetic prism separates the incoming unpolarized beam in two subbeams polarized parallel and antiparallel to the z axis, respectively.¹⁵

It will be assumed that the interferometer is positioned such that only the beam representing the $|\uparrow_z\rangle$ state satisfies the Bragg condition. (Here it is defined as the spin state reflected by the Heusler crystal.) The Schrödinger equation of neutrons in a static magnetic field is given by

$$\left[-\frac{\hbar^2}{2m} \nabla^2 - \mu \vec{\sigma} \cdot \vec{B} \right] \Psi = E_0 \Psi. \quad (A1)$$

Here $\mu \vec{\sigma} = \vec{\mu}$ is the operator of the magnetic moment of the neutrons. In the case of the guide fields $\vec{B} = B_0 \hat{z}$. As $\mu B_0/E_0$ was of magnitude 10^{-8} , for the wave vectors \vec{K}_{\pm} resulting from Eq. (A1) the approximation

$$\vec{K}_{\pm} \sim \vec{k} \left[1 \pm \frac{\mu B_0}{2E_0} \right] \quad (A2)$$

can be made. Neglecting an arbitrary phase factor and introducing $\vec{\kappa} \equiv \mu B_0 \vec{k}/2E_0$, the spinor wave function of the incident beam can be written as

$$\Psi_i = \begin{pmatrix} e^{-i\vec{\kappa} \cdot \vec{r}} \\ 0 \end{pmatrix} e^{i\vec{k} \cdot \vec{r}}. \quad (A3)$$

The polarization of the incident beam is

$$\vec{P}_i = \Psi_i^* \vec{\sigma} \Psi_i / \Psi_i^* \Psi_i = (0, 0, +1).$$

2. Coil operators

Similar to spin-echo systems²⁶ matrix formalism is chosen to describe the action of the dc coils on the neutron state. A rectangular dc coil represents a region of length l with a static homogeneous magnetic field $\vec{B}_f = B_f \hat{e}$ along the neutron trajectory. Its effect upon the spinor wave function can therefore be calculated solving Eq. (A1) for the case of general field direction. As a result a unitary operator \hat{U} can be assigned to a dc coil, when the assumption of zero reflection at the boundaries of the field region is used.¹¹ Ψ_a denoting the spinor before and Ψ_b being the spinor behind the field one gets

$$\Psi_b = \hat{U} \Psi_a$$

with

$$\begin{aligned} \hat{U} &= \exp \left[-i \frac{\vec{\sigma}}{2} \cdot \hat{e} k \frac{\mu B_f l}{2E_0} \right] \\ &= \exp(-i \vec{\sigma} \cdot \vec{\alpha} / 2). \end{aligned} \quad (\text{A4})$$

Here $\hat{e} = (e_x, e_y, e_z)$ is the unit vector of the field direction. In deriving the above operator the same approximation as in Eq. (A2) could be made, as the field strength inside the dc coils was of equal magnitude as in the guide field. The product in the exponent of Eq. (A4) was transformed using the Larmor frequency $\omega_L = (2\mu/\hbar)B_f$, the velocity of the incident neutrons $v = \hbar k/m$, the interval $\tau = l/v$ the time the neutrons need to traverse the field region, and the definition $\vec{\alpha} \equiv \hat{e} \omega_L \tau$. Also it was assumed that the time of flight τ in the field is the same for neutrons of both spin states²⁷: $\tau_+ = l/v_+$, $\tau_- = l/v_-$, and $\tau_+ \sim \tau_- \sim \tau$. Equation (A4) reflects the well-known property that the effect of a magnetic field region upon the spinor can be interpreted as that of a rotation of a system with spin $\frac{1}{2}$. Now the individual operators as represented by the different coils shall be calculated. The field region of the spin flipper consists of two parts. Their combined action can be understood as a rotation of π around some axis in the x - y plane.¹⁸ As long as the axis lies within this plane, its exact direction is not relevant for the purpose of inverting the polarization from $+z$ to $-z$. For the sake of simplicity a rotation around $+x$ is assumed. But instead of the ideal angle of π a more realistic one, namely, $\pi + \epsilon$ will be chosen. By doing this, not an exact transformation from the $|\uparrow_z\rangle$ state to the $|\downarrow_z\rangle$ state is obtained, but the beam after the spin flipper will be represented by a wave function containing both states. On the one hand this describes the action of the real

spin flipper more accurately, as ϵ is some constant angle caused by inexact coil geometry and maladjustment of dc currents. On the other hand, the consideration becomes more general, showing that to observe phenomena of spin superposition it suffices that the spins in beam I be not parallel to those in beam II. Thus the operator of the spin flipper reads as

$$\begin{aligned} \hat{U}_{sf}^{\text{real}} &= \exp[-i\sigma_x(\pi + \epsilon)/2] \\ &= \begin{pmatrix} \cos\left[\frac{\pi + \epsilon}{2}\right] & -i \sin\left[\frac{\pi + \epsilon}{2}\right] \\ -i \sin\left[\frac{\pi + \epsilon}{2}\right] & \cos\left[\frac{\pi + \epsilon}{2}\right] \end{pmatrix}. \end{aligned} \quad (\text{A5})$$

The accelerator coil can be looked at as a region where the strength of the guide field can be varied. Therefore the corresponding operator has the effect of a rotation around $+z$ by some angle α ,

$$\hat{U}_{\text{acc}} = \exp\left[-i\sigma_z \frac{\alpha}{2}\right] = \begin{pmatrix} e^{-i\alpha/2} & 0 \\ 0 & e^{i\alpha/2} \end{pmatrix}. \quad (\text{A6})$$

It should be noted that the guide field along the neutron trajectories, too, could be described by a series of rotations around $+z$. As will be seen later, this would only give additional phase factors in the observed intensity oscillations which, as constants throughout the whole experiment, have no influence on the result. The $\pi/2$ coil causes a rotation around $+x$ (or some axis in the x - y plane) by an angle of $\pi/2$. The operator is

$$\begin{aligned} \hat{U}_{\pi/2} &= \exp\left[-i\sigma_x \frac{\pi}{2}\right] \\ &= \frac{1}{\sqrt{2}} \begin{pmatrix} 1 & -i \\ -i & 1 \end{pmatrix}. \end{aligned} \quad (\text{A7})$$

3. Wave function

Using the operators presented above the expressions for the intensity can be derived in a straightforward way. The wave functions of beams I and II immediately after the first slab of the interferometer have the form

$$\begin{aligned} \Psi_{\text{I}} &= t \begin{pmatrix} e^{-iky} \\ 0 \end{pmatrix} e^{iky}, \\ \Psi_{\text{II}} &= r \begin{pmatrix} e^{-iky} \\ 0 \end{pmatrix} e^{iky}. \end{aligned} \quad (\text{A8})$$

Here the transmission and reflection amplitudes of

the crystal slab are introduced. They obey the relation $|r|^2 + |t|^2 = 1$, as there is practically no absorption for thermal neutrons in the Si single crystal.¹⁹⁻²¹ Furthermore, the fact that the wave trains have different direction inside the interferometer is neglected and the consideration is reduced to one dimension, which we call the y axis and which is parallel to the incident beam. This can be done because the absolute values of the wave numbers are the same in the transmitted and reflected directions. Then the nuclear phase shift χ of beam II relative to beam I is caused by the aluminum phase plate. χ can be varied rotating the plate. At the second slab both beams experience a reflection. Afterwards, Ψ_I is subject to the rotation. The spinor behind the spin flipper becomes

$$\begin{aligned} \Psi_I &\rightarrow \hat{U}_{sf}^{real} \Psi_I \\ &= tr \begin{pmatrix} \delta e^{-iky} \\ -i(1-\delta^2)^{1/2} e^{iky} \end{pmatrix} e^{iky - iky_{sf}} \end{aligned}$$

with

$$\vec{P}_I = \frac{\Psi_I^* \vec{\sigma} \Psi_I}{\Psi_I^* \Psi_I} = \begin{pmatrix} 2\delta(1-\delta^2)^{1/2} \sin 2\kappa y \\ -2\delta(1-\delta^2)^{1/2} \cos 2\kappa y \\ -1 + 2\delta^2 \end{pmatrix} \xrightarrow{\delta \rightarrow 0} \begin{pmatrix} 0 \\ 0 \\ -1 \end{pmatrix},$$

$$\vec{P}_{II} = \frac{\Psi_{II}^* \vec{\sigma} \Psi_{II}}{\Psi_{II}^* \Psi_{II}} = \begin{pmatrix} 0 \\ 0 \\ +1 \end{pmatrix}.$$

(A11)

For an ideal spin flip, opposite polarization of the beams can be produced.

After superposition in the third slab one obtains for the wave function in forward direction,

$$\Psi_0 = r^* \Psi_I + t \Psi_{II} = tr^* r \begin{pmatrix} (\delta + e^{i\chi}) e^{-iky} \\ -i(1-\delta^2)^{1/2} e^{iky} \end{pmatrix} e^{iky}. \quad (A12)$$

Its polarization is given by

$$P_0 = \frac{1}{(1 + \delta \cos \chi)} \begin{pmatrix} (1-\delta^2)^{1/2} [\delta \sin 2\kappa y + \sin(2\kappa y - \chi)] \\ -(1-\delta^2)^{1/2} [\delta \cos 2\kappa y + \cos(2\kappa y - \chi)] \\ \delta^2 + \delta \cos \chi \end{pmatrix} \xrightarrow{\delta \rightarrow 0} \begin{pmatrix} \sin(2\kappa y - \chi) \\ -\cos(2\kappa y - \chi) \\ 0 \end{pmatrix}. \quad (A13)$$

If one compares Eq. (A11) with Eq. (A13) the very different properties of the wave function after superposition become obvious, especially the influence of the phase shift χ on the polarization. The subsequent passage of the beam through the accelerator and the $\pi/2$ coils and the reflection at the Heusler crystal afford an analysis of this polarization. The wave function behind the $\pi/2$ coil is obtained by the transformation

$$\Psi_0 \rightarrow \hat{U}_{\pi/2} (\hat{U}_{acc} \Psi_0) = \frac{1}{\sqrt{2}} tr^* r \begin{pmatrix} (\delta + e^{i\chi}) e^{-iky'} e^{-i\alpha/2} - (1-\delta^2)^{1/2} e^{iky'} e^{i\alpha/2} \\ -i(\delta + e^{i\chi}) e^{-iky'} e^{-i\alpha/2} - i(1-\delta^2)^{1/2} e^{iky'} e^{i\alpha/2} \end{pmatrix} e^{iky}. \quad (A14)$$

Here the phase factors $\exp(\pm iky')$, which are determined by the exact location of the $\pi/2$ coil, can be set to 1, since their action can formally be incorporated into that of the accelerator coil.

The Heusler crystal reflects only neutrons of the $|\uparrow_z\rangle$ state into the detector with a reflectivity q and can

$$\delta = \cos \left[\frac{\pi + \epsilon}{2} \right]. \quad (A9)$$

Here y_{sf} denotes the entrance boundary from the guide field to the spin-flip field. As an experimental constant the associated phase factor can be set equal to 1. δ is the deviation from an exact spin flip that vanishes if $\epsilon = 0$. Taking now into account the property that the reflectivity on one side of a lossless mirror is the complex conjugate of the reflectivity when reflecting on the other side,²⁸ the spinors just before entering the third crystal slab can be written as

$$\begin{aligned} \Psi_I &= tr \begin{pmatrix} \delta e^{-iky} \\ -i(1-\delta^2)^{1/2} e^{iky} \end{pmatrix} e^{iky}, \\ \Psi_{II} &= r^* r \begin{pmatrix} e^{-iky} \\ 0 \end{pmatrix} e^{iky + i\chi}. \end{aligned} \quad (A10)$$

Now it may be well to look at the polarization of these individual beams,

therefore be symbolized by an appropriate projection operator. The final intensity in the detector turns out to be

$$\begin{aligned}
 I_0 &= \frac{1}{2} |qtr^*r| |e^{-i\alpha}(\delta + e^{i\chi}) - (1 - \delta^2)^{1/2}|^2 \\
 &= |qtr^*r| [1 + \delta \cos\chi - \delta(1 - \delta^2)^{1/2} \cos\alpha - (1 - \delta^2)^{1/2} \cos(\alpha - \chi)] \\
 &\xrightarrow{\delta \rightarrow 0} |qtr^*r|^2 [1 - \cos(\alpha - \chi)]. \tag{A15}
 \end{aligned}$$

Here four characteristic contributions can be distinguished. The first term in square brackets is the average intensity. The second term shows oscillations stemming from the superposition of components of equal spin state of beams I and II; it only depends on the nuclear phase shift χ . The third term accounts for an incomplete spin flip. Coming only from beam I it cannot depend on the nuclear phase shift, but it depends on the action of the accelerator coil (α). It can be imagined as Larmor pre-

cession of the remaining x - y components in beam I. Both the second and third terms disappear if an ideal spin flip can be achieved. The fourth term is the contribution by the superposition of opposite spin states we are looking for. It exhibits an equivalence of scalar phase shift inside (χ) and controlled Larmor precession (α) behind the interferometer. This feature cannot be explained if strict incoherence (i.e., mixture) of spin states $|\uparrow_z\rangle$ and $|\downarrow_z\rangle$ is expected.

¹*Neutron Interferometry*, edited by U. Bonse and H. Rauch (Clarendon, Oxford, 1979).

²W. Bauspiess, U. Bonse, and H. Rauch, *Nucl. Instrum. Methods* **157**, 495 (1978).

³H. Kaiser, H. Rauch, W. Bauspiess, and U. Bonse, *Z. Phys.* **A291**, 231 (1979).

⁴S. Hammerschmied, H. Rauch, H. Clerc, and U. Kischko, *Z. Phys.* **A302**, 323 (1981).

⁵R. Collela, A. W. Overhauser, and S. A. Werner, *Phys. Rev. Lett.* **34**, 1472 (1975).

⁶H. Rauch, H. Wilfing, A. Zeilinger, W. Bauspiess, and U. Bonse, *Z. Phys.* **B29**, 281 (1978).

⁷H. Rauch, A. Zeilinger, G. Badurek, A. Wilfing, W. Bauspiess, and U. Bonse, *Phys. Lett.* **54A**, 425 (1975).

⁸S. A. Werner, R. Collela, A. W. Overhauser, and C. F. Eagen, *Phys. Rev. Lett.* **35**, 1053 (1975).

⁹G. Badurek, H. Rauch, A. Zeilinger, W. Bauspiess, and U. Bonse, *Phys. Rev. D* **14**, 1177 (1976).

¹⁰E. P. Wigner, *Am. J. Phys.* **31**, 6 (1963).

¹¹G. Eder and A. Zeilinger, *Nuovo Cimento B* **34**, 76 (1976); A. Zeilinger, *Z. Phys. B* **25**, 97 (1976).

¹²A. Zeilinger, in Ref. 1, p. 241.

¹³J. Summhammer, G. Badurek, H. Rauch, and U. Kischko, *Phys. Lett.* **90A**, 110 (1982).

¹⁴W. Just, C. S. Schneider, P. Ciszewski, and C. G. Shull, *Phys. Rev. B* **7**, 4142 (1973).

¹⁵G. Badurek, H. Rauch, A. Wilfing, U. Bonse, and W. Graeff, *J. Appl. Crystallogr.* **12**, 186 (1979).

¹⁶T. Rekveldt, *J. Phys. (Paris) Colloq.* **32**, C579 (1971).

¹⁷F. Mezei, *Z. Phys.* **255**, 146 (1972).

¹⁸J. Summhammer, Ph.D. thesis Technical University of Vienna, 1982 (unpublished).

¹⁹U. Bonse and W. Graeff, *Top. Appl. Phys.* **22**, 93 (1977).

²⁰D. Petrascheck, *Acta Phys. Austriaca* **45**, 217 (1976).

²¹H. Rauch and D. Petrascheck, *Top. Curr. Phys.* **6**, 303 (1978).

²²A. Zeilinger and C. G. Shull, *Phys. Rev. B* **19**, 3957 (1979).

²³G. Badurek, H. Rauch, and A. Zeilinger, *Z. Phys.* **38**, 303 (1980).

²⁴H. Kendrick, J. S. King, S. A. Werner, and A. Arrot, *Nucl. Instrum. Methods* **79**, 82 (1970).

²⁵E. Balcar, in Ref. 1, p. 252.

²⁶J. B. Hayter, *Z. Phys.* **B31**, 117 (1978).

²⁷H. J. Bernstein and A. Zeilinger, *Phys. Lett.* **75A**, 169 (1980).

²⁸A. Zeilinger, *Am. J. Phys.* **49**, 882 (1981).